Naturally occurring anthraquinones as potential inhibitors of SARS-CoV-2 main protease: A molecular docking study

Sourav Das and Atanu Singha Roy*

Department of Chemistry, National Institute of Technology Meghalaya, Shillong 793003, India

Running Head Title: Anthraquinones as potential inhibitors of SARS-CoV-2 M^{pro}

***Corresponding Author:** Atanu Singha Roy

Tel.: +91 364−2501294

Fax: +91 364−2501113

Email: singharoyatanu@gmail.com; asroy86@nitm.ac.in

Abstract

Background: The novel coronavirus (COVID-19) has quickly spread throughout the globe, affecting millions of people. The World Health Organization (WHO) has recently declared this infectious disease as a pandemic. At present, several clinical trials are going on to identify possible drugs for treating this infection. SARS-CoV-2 M^{pro} is one of the most critical drug targets for the blockage of viral replication.

Method: The blind molecular docking analyses of natural anthraquinones with SARS-CoV-2 M^{pro} were carried out in an online server, SWISSDOCK, which is based on EADock DSS docking software.

Results: Blind molecular docking studies indicated that several natural antiviral anthraquinones could prove to be effective inhibitors for SARS-CoV-2 M^{pro} of COVID-19 as they bind near the active site having the catalytic dyad, HIS41 and CYS145 through non-covalent forces. The anthraquinones showed less inhibitory potential as compared to the FDA approved drug, remdesivir.

Conclusion: Among the natural anthraquinones, alterporriol Q could be the most potential inhibitor of SARS-CoV-2 M^{pro} among the natural anthraquinones studied here, as its ΔG value differed from that of remdesivir only by 0.51 kcal/ mol. The uses of these alternate compounds might be favorable for the treatment of the COVID-19.

Keywords: Remdesivir; anthraquinones; SARS-CoV-2 M^{pro}; COVID-19; molecular docking

1. Introduction

December 2019, saw the emergence of an array of severe pneumonia cases caused by coronavirus (CoV) in the city of Wuhan, China [1]. CoV is an enveloped positive-stranded RNA virus, portrayed by club-like spikes on their surface and belongs to the group *Cornonaviridae* of the *Nidovirales* order [2]. The genomic sequencing of the 2019 CoV showed that it is 96.2% alike to a bat coronavirus and shares 79.5% sequence similarity to SARS-CoV [3], hence the International Committee on Taxonomy of Viruses named this novel coronavirus as severe acute respiratory syndrome coronavirus 2 (SARS-CoV-2), and the associated pneumonia was named as COVID-19 by the World Health Organization (WHO) on the 11th of February, 2020. The pandemic has spread to more than 210 countries affecting a population of 33,49,786 and leading to the death of 2,38,628 as on 3rd May, 2020 [4]. Even after four months, no specific antivirals or clinically effective vaccines are available for the treatment and prevention of COVID-19. As COVID-19 is absolutely new to the immune system of humans, people throughout the globe are at risk of becoming sick on exposure to SARS-CoV-2 [5]. Therefore, considering the global threat due to this viral infection, there is a serious need to find out a vaccine/antiviral to treat this viral infection in order to reduce the transmission. Several drugs such as hydroxychloroquine [6], remdesivir, chloroquine [7], favipiravir [8,9], and ivermectin [10] but under clinical trial only remdesivir has shown potential for the treatment of COVID-19. SARS-CoV-2 contains the main protease (M^{pro}) also known as 3C-like protease ($3CL^{pro}$), which consists of a highly conserved catalytic domain from the SARS virus and is essential for controlling several functions of the CoV [11]. One vital function is the replication of the virus making it one of the best characterized target for drug development, hence targeting the M^{pro} would prevent the virus from building its proteins [12]. SARS-CoV-2 M^{pro} (Figure 1), is a three-domain (I to III) cysteine protease and is a homodimer. The domain I (8-101) and II (102-184) consists of β-barrels

mostly, and III (201-306) is made up of mainly of α-helices [13]. The structure consists of a conserved non-canonical HIS41-CYS145 dyad located within the cleft between domains I and II [3].

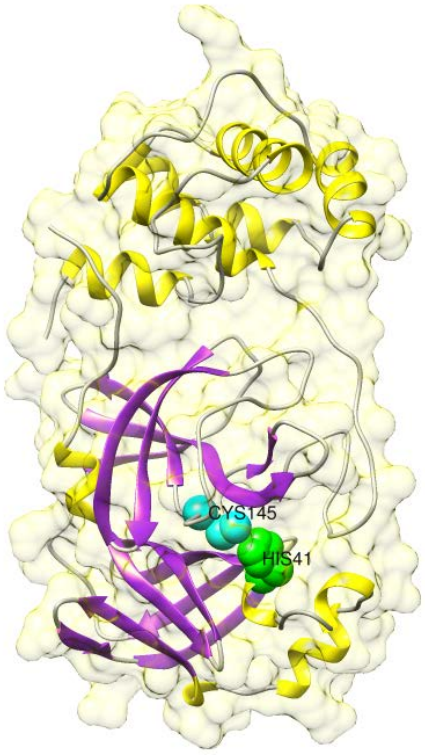

Figure 1: Native crystal structure of main protease of SARS-CoV-2 (PDB ID: 6y84) highlighting the conserved catalytic dyad, HIS41 and CYS145 as green and cyan spheres, respectively.

Natural anthraquinones are a class of aromatic compounds having low toxicity and high bioactivity [14,15]. One of the important properties of anthraquinones is based on their antiviral activity [16,17], which in the current context of COVID-19 pandemic is needed to be analyzed for their inhibitory potential against the SARS-CoV-2 infection. Here, in this report, we have reported the inhibitory potentials of 13 naturally occurring anthraquinones such as emodin, aloe emodin, chrysophanic acid, Tetrahydroaltersolanol C, aloin A and B, rhein, rubiadin, alterporriol Q, damnacanthal, hypericin, pseudohypericin and isopseudohypericin against SARS-CoV-2 M^{pro}

through blind molecular docking analysis and compared their results with the currently claimed anti COVID-19 drug remdesivir. The antiviral activities of the above mentioned natural anthraquinones along with their sources, are listed in the Table S1. It is to be noted that isopseudohypericin has not been reported for its antiviral property till date, but as *Hypericum perforatum* extract has antiviral effects [18], and isopseudohypericin is isolated from *Hypericum perforatum;* therefore it might have antiviral effect, hence we studied its binding efficacy with SARS-CoV-2 M^{pro}. This work concentrates on the recognition of natural anthraquinones compounds with a particular objective to accelerate the process of identification of specific/alternate drugs for COVID-19 treatment.

2. Methods

Blind molecular docking method has become an increasingly essential technique for drug discovery and understanding protein-ligand interactions. The blind docking procedures carry out an unbiased search over the entire surface of the protein/enzyme for the identification of binding sites. Hence, blind molecular docking studies of several natural antiviral anthraquinones were carried out with SARS-CoV-2 $M^{pro,}$ and their results were compared with that of remdesivir.

2.1. Geometry optimization of the compounds

The 3D co-ordinates of the compounds, remdesivir, emodin, aloe emodin, chrysophanic acid, tetrahydroaltersolanol C, aloin A and B, rhein, rubiadin, alterporriol Q, damnacanthal, hypericin, pseudohypericin and isopseudohypericin were downloaded as a .mol file from ChemSpider (www.chemspider.com) and geometry optimized further using the Parametric Method 3 (PM3) in ArgusLab [19,20]. The optimized structures of remdesivir and the natural anthraquinones are

depicted in the Figure S1. The ChemSpider ID of the compounds are listed in the Table S1, and the *logP* values obtained from SwissADME [21] analysis are included in the Table 1.

2.2. Molecular docking analyses and visualization

The 3D crystal structure of SARS-CoV-2 M^{Pro} (PDB ID. 6Y84) was downloaded from Protein Data Bank (PDB) [22]. Molecular docking study on a single chain was carried out by removing the water molecules from the PBD using PyMOL [23]. The final PDB file of M^{pro} and optimized ligands using ArgusLab were directly fed into an online docking server, SwissDock (http://www.swissdock.ch/docking). SwissDock incorporates an automated in silico molecular docking procedure based on EADock DSS docking algorithm which utilizes the CHARMM (Chemistry at HARvard Macromolecular Mechanics) forcefield [24]. According to SwissDock the minimum energy docked conformers are ranked in terms of their fullfitness score. The docked pose that has the least fullfitness score is used for further analysis. The molecular visualization were carried out using UCFS Chimera [25], PyMOL [23] and the 2D interaction plots were created using Discovery Studio Visualizer [26]. The online server available at http://cib.cf.ocha.ac.jp/bitool/ASA/ was used to calculate the changes in the accessible surface area (ΔASA) of the M^{pro} protease on interactions with the compounds.

3. Results and Discussion

The fullfitness score free energy of binding and the *logP* values of the control drug, remdesivir and that of the 13 natural anthraquinones have been listed in the Table 1. From this Table 1, it could be observed that the estimated ΔG is higher for remdesivir (-8.99 kcal/mol) as compared to all the anthraquinones, which means that the inhibitory potency of these anthraquinones is lesser than that of the control drug. But alterporriol Q (-8.48 kcal/mol) has very close ΔG value to that

of remdesivir, while others have energies in between 6.64-7.75 kcal/mol. The *logP* values listed in the Table 1 measures the molecular hydrophobicity or lipophilicity of a particular compound. High *logP* values show poor absorption or low permeability, whereas low *logP* values are indication of high absorption and permeability. A *logP* value greater than 5, indicates a high hydrophobic character of a compound [27]. Here, the *logP* values of most of the anthraquinones are less than 5 and, excluding only hypericin. The *logP* values are very important for the understanding of how the compounds may penetrate cell membranes. Unfortunately, a relationship between the estimated binding energy and the *logP* values could not be obtained here.

Table 1: Obtained parameters of the compounds corresponding to the minimum docked poses of remdesivir and the respective anthraquinones with SARS-CoV-2 M^{pro}.

S. No.	**Compound(s)**	**Fullfitness score (kcal/mol)**	**Estimated ΔG (kcal/mol)**	***logP***
1	Remdesivir	-1294.81	**-8.99**	2.21
2	Emodin	-1245.82	-6.90	1.89
3	Aloe-emodin	-1231.69	-7.12	1.21
4	Chrysophanic acid	-1230.25	-6.83	2.18
5	Tetrahydroaltersolanol C	-1226.14	-7.38	0.44
6	Aloin A	-1147.83	-7.75	-1.04
7	Aloin B	-1144.11	-7.64	-1.04
8	Rhein	-1235.99	-7.00	1.57
9	Rubiadin	-1233.93	-6.64	2.18
10	Alterporriol Q	-1175.10	**-8.48**	3.70
11	Damnacanthal	-1209.40	-7.16	1.99

12	Hypericin	-1145.42	-7.18	5.39
13	Pseudohypericin	-1143.87	-7.26	4.42
14	Isopseudohypericin	-1171.30	-7.23	4.73

The minimum energy docked poses along with the 2D interaction plots of the compounds within the substrate-binding site of SARS-CoV-2 M^{pro} is depicted in the Figure 2. The nearby residues interacting with the compounds through non-covalent forces, except the van der Waals forces of attraction (shown in the 2D interaction plots) are also listed in the Table 2. It could be observed from Figure 2, that remdesivir and all the natural anthraquinones could bind to the active site of SARS-CoV-2 M^{pro} which is lined up by residues such as THR25, THR26, HIS41, MET49, GLY143, CYS145, GLU166, PRO168, etc. A recent study by Zhang et al. (2020) [28], have indicated the importance of the two catalytic residues HIS41 and CYS145, and other residues like GLY143, CYS145, HIS163, HIS164, GLU166, PRO168, and GLN189 for the design of α-ketoamide inhibitors for SARS-CoV-2 M^{pro}. Similarly, Dai et al. (2020) [3], have also shown the importance of these residues for the design and synthesis of antiviral compounds as inhibitors of SARS-CoV-2 M^{pro}. Therefore, the natural anthraquinones studied here could inhibit the viral disease by binding to the active site of M^{pro}.

The compound stabilize within the active site of M^{pro} by different non-covalent forces such as hydrogen-bonding, π-alkyl, π-sigma, π-π stacked interactions, and others as shown in the 2D interaction plots of Figure 2. The stability of ligand within the binding site of a macromolecule is largely related to the hydrogen bonding interactions formed between the two counterparts [29,30]. Remdesivir forms two hydrogen bonds (H-bonds) with GLU166 (3.90 Å) and GLN189 (4.29 Å) (Figure 2a). Among the anthraquinones from Rhubarb, emodin (Figure 2b) forms H-bonds with THR25 (3.81 Å) and GLY143 (3.63 Å), rhein forms H-bonds with THR25 (3.65 Å),

GLY143 (3.73 Å) and GLU166 (3.97Å) (Figure 2c), while chrysophanic acid interacts with GLY143 through H-bonds at a distance of 3.61 Å (Figure 2d). For the anthraquinones from aloe (Figure 2e-g), aloe emodin forms H-bonds with PHE140 and GLY143 (3.57Å), aloin A forms two H-bonds with GLN189 at a distance of 3.89 and 3.76 Å, one each with CYS145 (4.95Å) and GLU166 (5.05 Å), while aloin B forms two H-bonds with ASN142.

Rubiadin, an anthraquinone from *Rubia Cordifolia,* forms H-bonds with HIS41 (3.14 Å) and SER46 (3.69 Å) as can be seen from Figure 2h. Anthraquinones from *Alternaria sp.* fungus, tetrahydroaltersolanol C (Figure 2i) interacts with CYS44 (4.09 Å) and CYS145 (3.74 Å) through H-bonds, while alterporriol Q (Figure 2j) forms H-bonds with ASN142 (3.66 Å), GLY143(4.22 Å) and GLU166 (4.08 Å). Damnacanthal, an anthraquinone of Noni, forms H-bond with GLY143 (3.77 Å) as seen from Figure 2k. The anthraquinones (Figure 2l-n) of Hypericum perforatum, hypericin forms two H-bonds with GLU166 at a distance of 4.87 and 4.83 Å, pseudohypericin interacts with GLY143 (3.69 Å) and GLN189 (3.55 Å) residues through H-bonds, while isopseudohypericin forms two H-bonds with GLU166 at a distance of 4.13 and 4.24 Å. Besides the H-bonds, the conformational energy of the interactions are minimized through other non-covalent forces such as π-sigma, π-π stacked, amide-π, π-alkyl, π-sulphur and van der Waals forces as shown in the 2D interactions plots of the docked poses of Figure 2 [31].

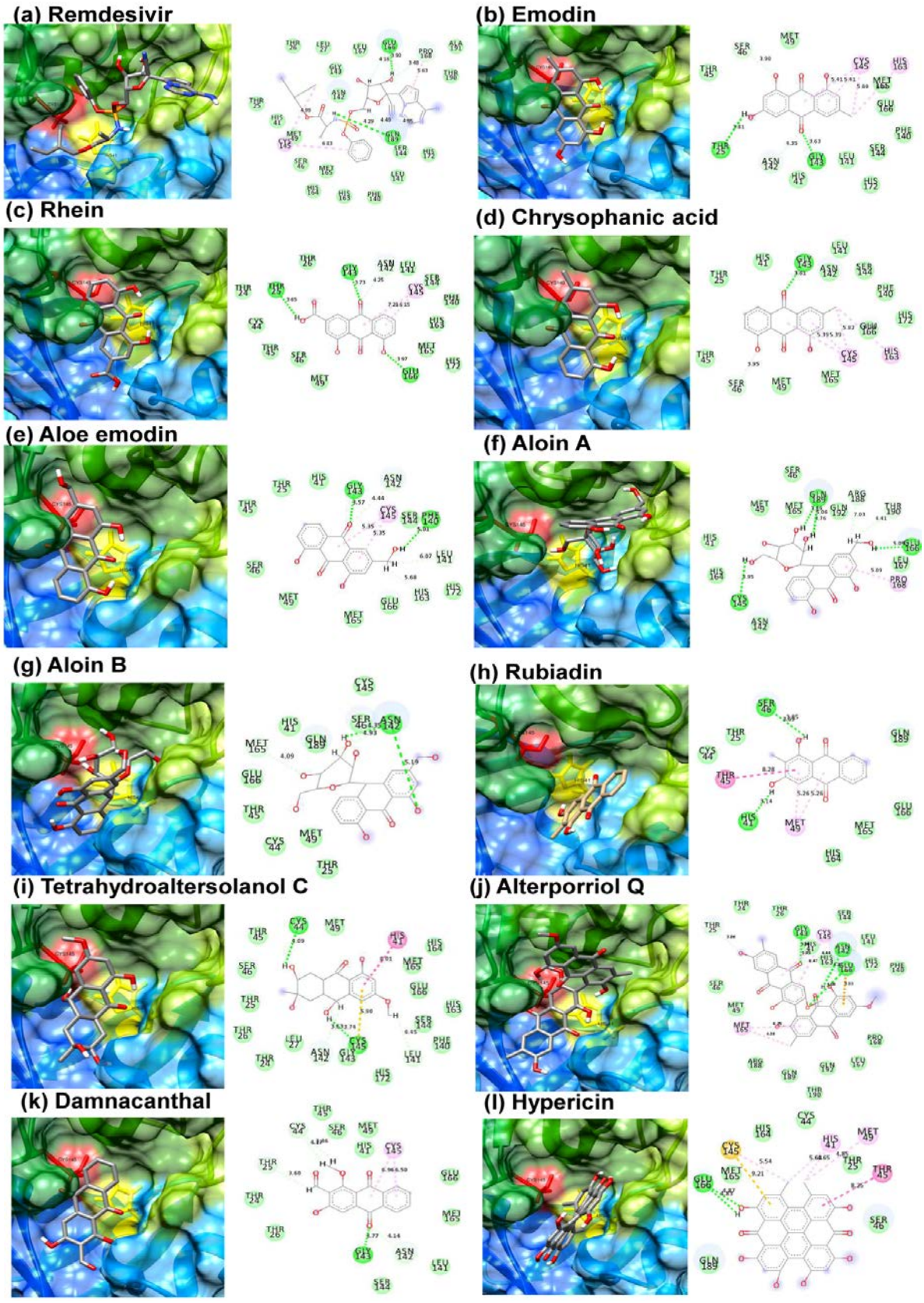
(a) Remdesivir
(b) Emodin
(c) Rhein
(d) Chrysophanic acid
(e) Aloe emodin
(f) Aloin A
(g) Aloin B
(h) Rubiadin
(i) Tetrahydroaltersolanol C
(j) Alterporriol Q
(k) Damnacanthal
(l) Hypericin

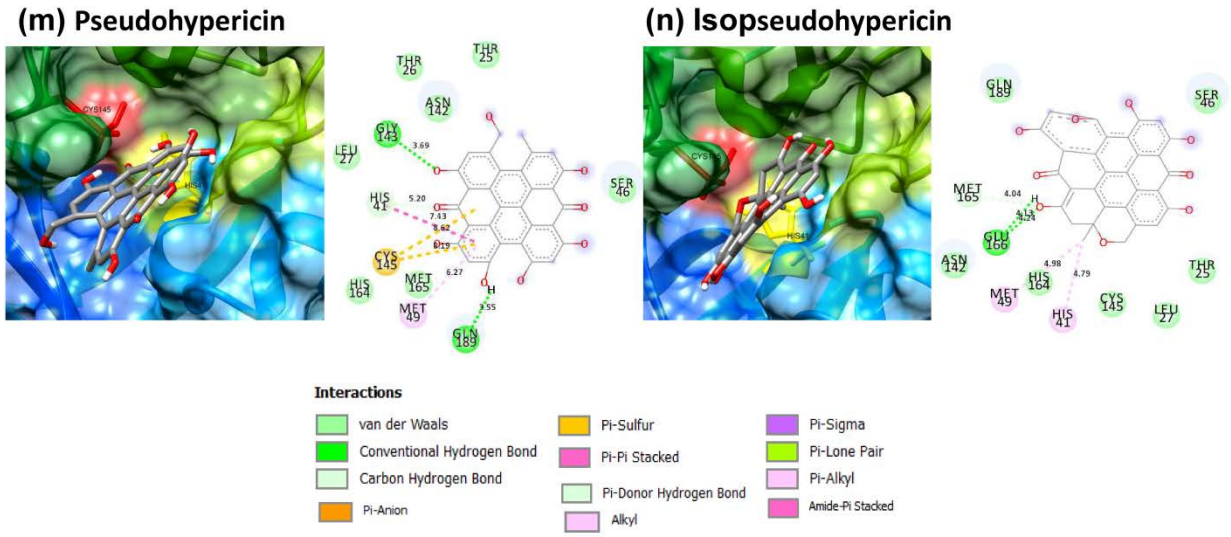

Figure 2. Docked poses of remdesivir and the anthraquinones within the active site of SARS-CoV-2 M^{pro} and their corresponding 2D interaction plots.

Table 2. The residues surrounding the binding site of the anthraquinone compounds within the active site of SARS-CoV-2 M^{pro}.

Compound(s)	**Interacting residues in the active site of SARS-CoV-2 M^{pro}**
Remdesivir	MET49, HIS41, CYS145, GLU166, PRO168, GLN189
Emodin	THR25, HIS41, GLY143, CYS145, HIS163
Aloe-emodin	HIS41, PHE140, ASN142, GLY143, CYS145, HIS163
Chrysophanic acid	HIS41, SER46, GLY143, CYS145, HIS163
Tetrahydroaltersolanol C	HIS41, CYS44, LEU141, CYS145
Aloin A	CYS145, GLU166, PRO168, ARG188, GLN189, THR190
Aloin B	ASN142, CYS145, MET165
Rhein	THR25, ASN142, GLY143, CYS145, GLU166
Rubiadin	HIS41, THR45, SER46, MET49
Alterporriol Q	THR25, HIS41, ASN142, GLY143, CYS145, HIS163, MET165, GLU166
Damnacanthal	THR25, CYS44, GLY143, CYS145
Hypericin	HIS41, THR45, MET49, CYS145
Pseudohypericin	HIS41, MET49, GLY143, CYS145, GLN189
Isopseudohypericin	HIS41, MET49, MET165, GLU166

Herein, the blind molecular docking studies of the natural anthraquinones with M^{pro} indicated that they possess inhibitory potential towards SARS-CoV-2, as they can bind to the substrate-binding site of SARS-CoV-2 M^{pro} which is essential for inhibiting the viral replication [28]. This substrate binding site of M^{pro} is lined up by residues such as HIS41, MET49, GLY143, CYS145, HIS163, HIS164, GLU166, PRO168, and GLN189. As HIS41 and CYS145 are the two important catalytic residues, therefore the distance of the compounds from these two residues along with the change in accessible area of the residues are listed in the Table 3. In terms of the estimated free energy of binding (ΔG) values, the control (remdesivir) has the highest affinity (-8.99 kcal/mol) to function as a potential inhibitor for SARS-CoV-2 M^{pro}, which indeed supports the promising role of remdesivir as a potential anti- COVID-19 drug on which the currently major research is going on throughout the world. Although, the none of the anthraquinones could cross that of the remdesivir inhibitory potential, but among the anthraquinones the inhibitory potential follows the following order alterporriol Q (-8.48 kcal/mol)> aloin A (-7.75 kcal/mol) > aloin B (-7.64 kcal/mol)> tetrahydroaltersolanol C (-7.38 kcal/mol) > pseudohypericin (-7.26 kcal/mol)> isopseudohypericin (-7.23 kcal/mol) >hypericin (-7.18 kcal/mol)> damnacanthal (-7.16 kcal/mol)> aloe emodin (-7.12 kcal/mol) > rhein (-7.00 kcal/ mol)> emodin (-6.90 kcal/mol)> chrysophanic acid (6.83 kcal/mol) >rubiadin (-6.64 kcal/mol).

Since 1972 onwards, the world has seen the emergence of more than 50 new viruses which been recognized as etiologic agents of human diseases [32]. The development of antiviral drugs is a time consuming and a complex phenomenon, hence the evolution of new viruses calls for the development and usage of efficient strategies to synthesize or identify already known antiviral drugs that limit the spread or treat the virus. Over the years, since the discovery of idoxuridine (IDU) in 1959 [32], several antivirals that affect the viruses life cycle have been determined

which lead to a number of antiviral protocols being proposed, that includes targeting intracellular signal transduction pathways or inhibiting the viral replication [32]. Though, a number of antivirals have been identified, only very few molecules have proven to be safe and effective when subjected to selective antiviral therapy. In the current context, the repurposing of FDA approved drugs or the use of compounds from natural sources is an essential concept due to its cost effectiveness and ease of availability in terms of research and development of new drugs, particularly at this junction where the COVID-19 pandemic is posing as a global threat. In addition to the FDA approved drug, remdesivir here we observed that the anthraquinones, particularly alterporriol Q posses significant inhibitory potential towards SARS-CoV-2 M^{pro}. Naturally occurring anthraquinones have low toxicity and different biological activities [14,33]. Therefore, these observations indicate a promising potential for the use of natural anthraquinones for the treatment of COVID-19.

Table 3: Change in accessible surface area and distance of remdesivir and the anthraquinones from the catalytic dyad (HIS41 and CYS145) of SARS-CoV-2 M^{pro} on binding with remdesivir and the natural anthraquinones.

Compound(s)	**Distance (Å)**		**ΔASA (Å^2)**	
	HIS41	**CYS145**	**HIS41**	**CYS145**
Remdesivir	4.98	4.99	21.09	21.88
Emodin	4.17	5.41	21.09	21.88
Chrysophanic acid	4.08	5.39	21.09	21.88
Aloe-emodin	4.07	5.35	21.09	21.88
Aloin A	2.61	4.95	12.81	15.68
Aloin B	3.89	3.67	19.27	17.85
Rhein	4.25	6.15	21.09	21.88
Rubiadin	3.14	5.06	19.73	7.17
Tetrahydroaltersolanol C	8.01	3.63	21.09	21.88

Alterporriol Q	4.07	5.85	21.09	21.88
Damnacanthal	4.26	6.50	21.09	21.88
Hypericin	3.65	5.54	20.30	17.54
Pseudohypericin	7.43	8.19	17.91	17.84
Isopseudohypericin	4.79	3.35	20.524	20.33

4. Conclusion

Blind molecular docking has been used for studying the inhibitory potentials of natural anthraquinones against SARS-CoV-2 M^{pro} of COVID-19. Around 13 hit natural anthraquinones reported here to have potential inhibitory effects against the SARS-CoV-2 main protease. Nevertheless, this study provides a foundation for computational drug discovery of new natural compounds to treat and reduce the transmission COVID-19. It was observed that the anthraquinones could bind to the substrate binding site of SARS-CoV-2 M^{pro} which contains the two important catalytic dyad, HIS41 and CYS145, important for blocking the viral replication of the virus and further spread of the infection. The anthraquinones stabilized within the active site through different non-covalent forces such as hydrogen bonding, π-sigma, π-alkyl, π-π stacked, amide-π stacked and van der Waals interactions. Although, the inhibitory potential of the natural anthraquinones were found to be lesser than that of remdesivir in terms of the estimated ΔG value, alterporriol Q could be the most potential inhibitor of SARS-CoV-2 M^{pro} among the natural anthraquinones studied here, as its ΔG value differed from that of remdesivir by 0.51 kcal/ mol. This study provides a lead to the possibility of natural anthraquinones being used as treatment for COVID-19, but as this study has been carried out using blind molecular docking method, detailed *in vivo* and *in vitro* experiments are required to be carried out to gauge the applicability and toxicity of these anthraquinones.

5. Acknowledgments

SS and ASR are indebted to NIT Meghalaya for providing research platform. SD is grateful to the TEQIP III, NIT Meghalaya for fellowship. The study is not supported by any funding agency.

6. Authors Declaration

No conflict of interest to declare. The authors approved this version of manuscript for submission.

7. Authors Contribution

Sourav Das: Conceptualization, Methodology, Investigation, Writing - original draft.

Atanu Singha Roy: Conceptualization, Methodology, Investigation, Writing-reviewing and editing.

8. References

[1] Huang C, Wang Y, Li X, Ren L, Zhao J, Hu Y, et al. Clinical features of patients infected with 2019 novel coronavirus in Wuhan, China. Lancet 2020;395:497–506. https://doi.org/10.1016/S0140-6736(20)30183-5.

[2] Fehr AR, Perlman S. Coronaviruses: An overview of their replication and pathogenesis. Coronaviruses Methods Protoc., Springer New York; 2015, p. 1–23. https://doi.org/10.1007/978-1-4939-2438-7_1.

[3] Dai W, Zhang B, Su H, Li J, Zhao Y, Xie X, et al. Structure-based design of antiviral drug candidates targeting the SARS-CoV-2 main protease. Science 2020. https://doi.org/10.1126/science.abb4489.

[4] Coronavirus disease (COVID-19) Situation Report-103. n.d.

[5] Rahimi F, Bezmin Abadi AT. Challenges of managing the asymptomatic carriers of SARS-CoV-2. Travel Med Infect Dis 2020:101677. https://doi.org/10.1016/j.tmaid.2020.101677.

[6] Gautret P, Lagier J-C, Parola P, Hoang VT, Meddeb L, Mailhe M, et al. Hydroxychloroquine and azithromycin as a treatment of COVID-19: results of an open-label non-randomized clinical trial. Int J Antimicrob Agents 2020:105949. https://doi.org/10.1016/j.ijantimicag.2020.105949.

[7] Wang M, Cao R, Zhang L, Yang X, Liu J, Xu M, et al. Remdesivir and chloroquine effectively inhibit the recently emerged novel coronavirus (2019-nCoV) in vitro. Cell Res 2020 303 2020;30:269–71. https://doi.org/10.1038/s41422-020-0282-0.

[8] Cai Q, Yang M, Liu D, Chen J, Shu D, Xia J, et al. Experimental Treatment with Favipiravir for COVID-19: An Open-Label Control Study. Engineering 2020. https://doi.org/10.1016/j.eng.2020.03.007.

[9] Khambholja K, Asudani D. Potential repurposing of Favipiravir in COVID-19 outbreak based on current evidence. Travel Med Infect Dis 2020:101710. https://doi.org/10.1016/j.tmaid.2020.101710.

[10] Caly L, Druce JD, Catton MG, Jans DA, Wagstaff KM. The FDA-approved Drug Ivermectin inhibits the replication of SARS-CoV-2 in vitro. Antiviral Res 2020:104787. https://doi.org/10.1016/j.antiviral.2020.104787.

[11] Hall DC, Ji H-F. A search for medications to treat COVID-19 via in silico molecular docking models of the SARS-CoV-2 spike glycoprotein and 3CL protease. Travel Med Infect Dis 2020:101646. https://doi.org/10.1016/j.tmaid.2020.101646.

[12] Magro G. SARS-CoV-2 and COVID-19: What are our options? Where should we focus

our attention on to find new drugs and strategies? Travel Med Infect Dis 2020:101685. https://doi.org/10.1016/j.tmaid.2020.101685.

[13] Khan SA, Zia K, Ashraf S, Uddin R, Ul-Haq Z. Identification of Chymotrypsin-like Protease Inhibitors of SARS-CoV-2 Via Integrated Computational Approach. J Biomol Struct Dyn 2020:1–13. https://doi.org/10.1080/07391102.2020.1751298.

[14] Chien SC, Wu YC, Chen ZW, Yang WC. Naturally occurring anthraquinones: Chemistry and therapeutic potential in autoimmune diabetes. Evidence-Based Complement Altern Med 2015. https://doi.org/10.1155/2015/357357.

[15] Malik EM, Müller CE. Anthraquinones As Pharmacological Tools and Drugs. Med Res Rev 2016;36:705–48. https://doi.org/10.1002/med.21391.

[16] Cohen PA, Hudson JB, Towers GHN. Antiviral activities of anthraquinones, bianthrones and hypericin derivatives from lichens. Experientia 1996;52:180–3. https://doi.org/10.1007/BF01923366.

[17] Barnard DL, Huffman JH, Morris JLB, Wood SG, Hughes BG, Sidwell RW. Evaluation of the antiviral activity of anthraquinones, anthrones and anthraquinone derivatives against human cytomegalovirus. Antiviral Res 1992;17:63–77. https://doi.org/10.1016/0166-3542(92)90091-I.

[18] Chen H, Muhammad I, Zhang Y, Ren Y, Zhang R, Huang X, et al. Antiviral Activity Against Infectious Bronchitis Virus and Bioactive Components of Hypericum perforatum L. Front Pharmacol 2019;10:1272. https://doi.org/10.3389/fphar.2019.01272.

[19] Thompson MA. Molecular docking using ArgusLab, an efficient shape-based search algorithm and the AScore scoring function. ACS Meet., 2004.

[20] Das S, Sarmah S, Lyndem S, Singha Roy A. An investigation into the identification of

potential inhibitors of SARS-CoV-2 main protease using molecular docking study. J Biomol Struct Dyn 2020:1–18. https://doi.org/10.1080/07391102.2020.1763201.

[21] Daina A, Michielin O, Zoete V. SwissADME: A free web tool to evaluate pharmacokinetics, drug-likeness and medicinal chemistry friendliness of small molecules. Sci Rep 2017;7. https://doi.org/10.1038/srep42717.

[22] Owen, C.D., Lukacik, P., Strain-Damerell, C.M., Douangamath, A., Powell, A.J., Fearon, D., Brandao-Neto, J., Crawshaw, A.D., Aragao, D., Williams, M., Flaig, R., Hall, D.R., McAuley, K.E., Mazzorana, M., Stuart, D.I., von Delft, F., Walsh MA. COVID-19 main protease with unliganded active site (2019-nCoV, coronavirus disease 2019, SARS-CoV-2). RCSB Protein Data Bank ID 6Y84 2020:3–7. https://doi.org/10.2210/pdb6Y84.

[23] Schrodinger LLC. The PyMOL Molecular Graphics System, Version 2.0 2017.

[24] Grosdidier A, Zoete V, Michielin O. SwissDock, a protein-small molecule docking web service based on EADock DSS. Nucleic Acids Res 2011;39:W270-7. https://doi.org/10.1093/nar/gkr366.

[25] Pettersen EF, Goddard TD, Huang CC, Couch GS, Greenblatt DM, Meng EC, et al. UCSF Chimera—A Visualization System for Exploratory Research and Analysis. J Comput Chem 2004;25:1605–12. https://doi.org/10.1002/jcc.20084.

[26] BIOVIA DS. Discovery studio visualizer, 2019. Dassault Systèmes, San Diego 2019.

[27] Ditzinger F, Price DJ, Ilie A-R, Köhl NJ, Jankovic S, Tsakiridou G, et al. Lipophilicity and hydrophobicity considerations in bio-enabling oral formulations approaches - a PEARRL review. J Pharm Pharmacol 2019;71:464–82. https://doi.org/10.1111/jphp.12984.

[28] Zhang L, Lin D, Sun X, Curth U, Drosten C, Sauerhering L, et al. Crystal structure of

SARS-CoV-2 main protease provides a basis for design of improved α-ketoamide inhibitors. Science (80-) 2020:eabb3405. https://doi.org/10.1126/science.abb3405.

[29] Chen D, Oezguen N, Urvil P, Ferguson C, Dann SM, Savidge TC. Regulation of protein-ligand binding affinity by hydrogen bond pairing. Sci Adv 2016;2:e1501240. https://doi.org/10.1126/sciadv.1501240.

[30] Szefler. Docking Linear Ligands to Glucose Oxidase. Symmetry (Basel) 2019;11:901. https://doi.org/10.3390/sym11070901.

[31] Arthur DE, Uzairu A. Molecular docking studies on the interaction of NCI anticancer analogues with human Phosphatidylinositol 4,5-bisphosphate 3-kinase catalytic subunit. J King Saud Univ - Sci 2019;31:1151–66. https://doi.org/10.1016/j.jksus.2019.01.011.

[32] Bryan-Marrugo OL, Ramos-Jiménez J, Barrera-Saldaña H, Rojas-Martínez A, Vidaltamayo R, Rivas-Estilla AM. History and progress of antiviral drugs: From acyclovir to direct-acting antiviral agents (DAAs) for Hepatitis C. Med Univ 2015;17:165–74. https://doi.org/10.1016/j.rmu.2015.05.003.

[33] Islam R, Mamat Y, Ismayil I, Yan M, Kadir M, Abdugheny A, et al. Toxicity of Anthraquinones: Differential Effects of *Rumex* Seed Extracts on Rat Organ Weights and Biochemical and Haematological Parameters. Phyther Res 2015;29:777–84. https://doi.org/10.1002/ptr.5317.

Supplementary Information

Naturally occurring anthraquinones as potential inhibitors of SARS-CoV-2 main protease: A molecular docking study

Sourav Das and Atanu Singha Roy*

Department of Chemistry, National Institute of Technology Meghalaya, Shillong 793003, India

Running Head Title: Anthraquinones as potential inhibitors of SARS-CoV-2 M^{pro}

***Corresponding Author:** Atanu Singha Roy

Tel.: +91 364−2501294

Fax: +91 364−2501113

Email: singharoyatanu@gmail.com; asroy86@nitm.ac.in

Figure S1

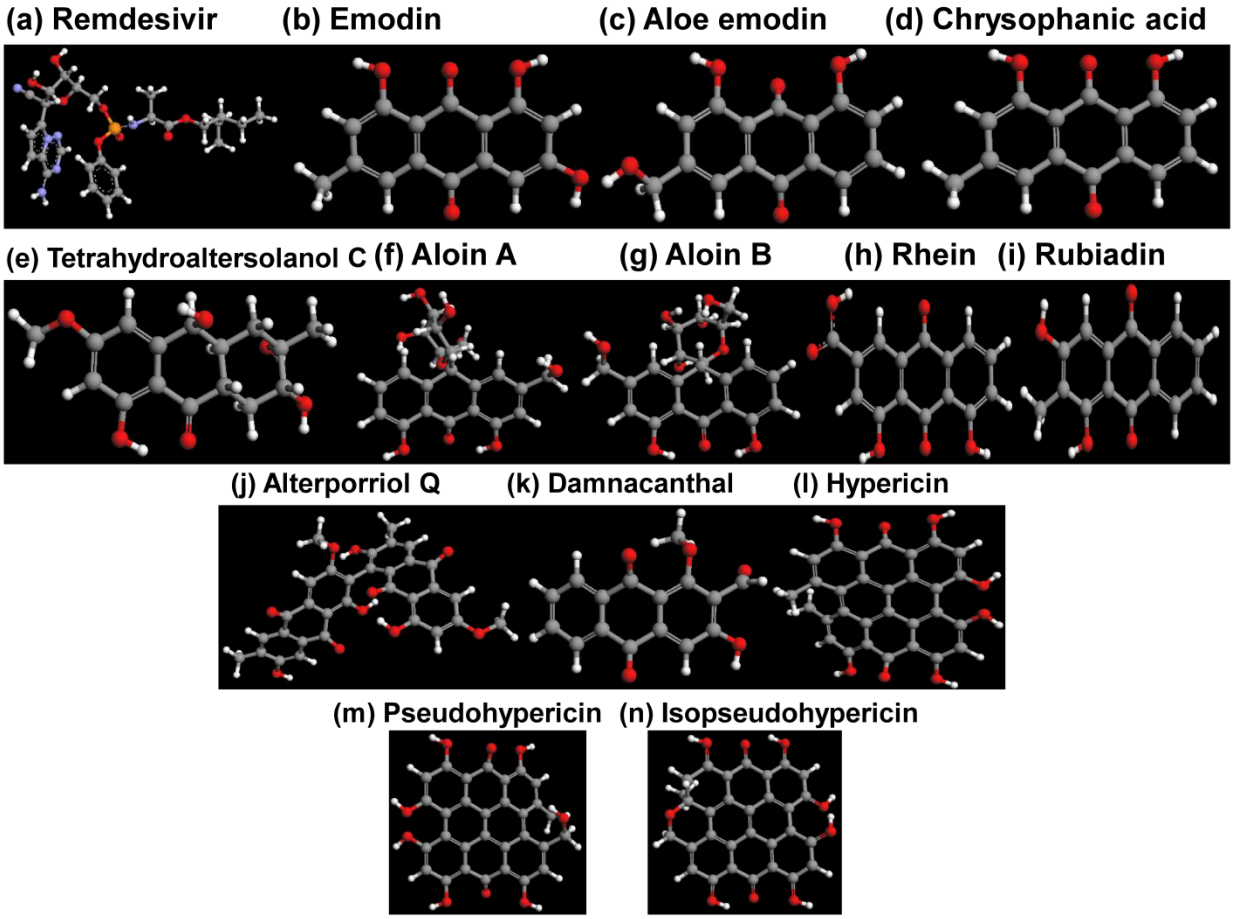

Figure S1. Geometry optimized structures of the compounds using PM3 method in ArgusLab.

Table S1. Biological properties and sources of the naturally occurring anthraquinones**.**

Anthraquinones	**ChemSpider ID**	**Biological activities**	**Sources**
Emodin	3107	Blocks the SARS coronavirus spike protein and angiotensin-converting enzyme 2 interaction [1]	Rhubarb [2]
Rhein	9762	Anti-influenza A virus activity [3]	Rhubarb [2]
Chrysophanic acid	9793	Against poliovirus [4]	Rhubarb [5]
Aloe emodin	9792	Against Japanese encephalitis virus and enterovirus 71 [6]	Aloe [7]
Aloin A	24534069	Effective against influenza viruses, including A(H1N1)pdm09 influenza viruses [9]	Aloe [7]
Aloin B	14269		Aloe [7]
Rubiadin	110563	Effective against hepatitis B virus [10]	Rubia Cordifolia [11]
Tetrahydroaltersolanol C	28504329	Effective against Porcine reproductive and respiratory syndrome virus (PRRSV) [12]	*Alternaria sp.* Fungus [13]
Alterporriol Q	28502063	Effective against Porcine reproductive and respiratory syndrome virus (PRRSV) [13]	*Alternaria sp.* Fungus [14]
Damnacanthal	2843	Inhibitor of HIV-1 Vpr induced cell death [15]	Noni [2]
Hypericin	4444511	Anti-IBV (Infectious Bronchitis virus) activity [16]	*Hypericum perforatum* [2]
Pseudohypericin	4445065	Anti-IBV (Infectious Bronchitis virus) activity [16]	*Hypericum perforatum* [17]
Isopseudohypericin	10192492		*Hypericum perforatum* [18]

References

[1] Ho TY, Wu SL, Chen JC, Li CC, Hsiang CY. Emodin blocks the SARS coronavirus spike protein and angiotensin-converting enzyme 2 interaction. Antiviral Res 2007;74:92–101. https://doi.org/10.1016/j.antiviral.2006.04.014.

[2] Li Y, Jiang JG. Health functions and structure-activity relationships of natural anthraquinones from plants. Food Funct 2018;9:6063–80. https://doi.org/10.1039/c8fo01569d.

[3] Wang Q-W, Su Y, Sheng J-T, Gu L-M, Zhao Y, Chen X-X, et al. Anti-influenza A virus activity of rhein through regulating oxidative stress, TLR4, Akt, MAPK, and NF-κB signal pathways. PLoS One 2018;13:e0191793. https://doi.org/10.1371/journal.pone.0191793.

[4] Semple SJ, Pyke SM, Reynolds GD, Flower RLP. In vitro antiviral activity of the anthraquinone chrysophanic acid against poliovirus. Antiviral Res 2001;49:169–78. https://doi.org/10.1016/S0166-3542(01)00125-5.

[5] Ko SK, Whang WK, Kim IH. Anthraquinone and stilbene derivatives from the cultivated Korean Rhubarb Rhizomes. Arch Pharm Res 1995;18:282–8. https://doi.org/10.1007/BF02976414.

[6] Lin CW, Wu CF, Hsiao NW, Chang CY, Li SW, Wan L, et al. Aloe-emodin is an interferon-inducing agent with antiviral activity against Japanese encephalitis virus and enterovirus 71. Int J Antimicrob Agents 2008;32:355–9. https://doi.org/10.1016/j.ijantimicag.2008.04.018.

[7] Park M-Y, Kwon H-J, Sung M-K. Intestinal absorption of aloin, aloe-emodin, and aloesin; A comparative study using two in vitro absorption models. Nutr Res Pract 2009. https://doi.org/10.4162/nrp.2009.3.1.9.

[8] Prinsloo G, Marokane CK, Street RA. Anti-HIV activity of southern African plants: Current developments, phytochemistry and future research. J Ethnopharmacol 2018. https://doi.org/10.1016/j.jep.2017.08.005.

[9] Huang CT, Hung CY, Hseih YC, Chang CS, Velu AB, He YC, et al. Effect of aloin on viral neuraminidase and hemagglutinin-specific T cell immunity in acute influenza. Phytomedicine 2019;64:152904. https://doi.org/10.1016/j.phymed.2019.152904.

[10] Peng Z, Fang G, Peng F, Pan Z, Su Z, Tian W, et al. Effects of Rubiadin isolated from Prismatomeris connata on anti-hepatitis B virus activity in vitro. Phyther Res 2017;31:1962–70. https://doi.org/10.1002/ptr.5945.

[11] Tripathi YB, Sharma M, Manickam M. Rubiadin, a new antioxidant from Rubia cordifolia. Indian J Biochem Biophys 1997.

[12] Zhang S-L, Wu Y-C, Cheng F, Guo Z-Y, Chen J-F. Anti-PRRSV effect and mechanism of tetrahydroaltersolanol C *in vitro*. J Asian Nat Prod Res 2016;18:303–14. https://doi.org/10.1080/10286020.2015.1072516.

[13] Zheng CJ, Shao CL, Guo ZY, Chen JF, Deng DS, Yang KL, et al. Bioactive hydroanthraquinones and anthraquinone dimers from a soft coral-derived Alternaria sp. fungus. J Nat Prod 2012;75:189–97. https://doi.org/10.1021/np200766d.

[14] Xu WF, Hou XM, Yang KL, Cao F, Yang RY, Wang CY, et al. Nigrodiquinone a, a hydroanthraquinone dimer containing a rare C-9-C-7' linkage from a zoanthid-derived Nigrospora sp. fungus. Mar Drugs 2016. https://doi.org/10.3390/md14030051.

[15] Kamata M, Wu RP, An DS, Saxe JP, Damoiseaux R, Phelps ME, et al. Cell-based chemical genetic screen identifies damnacanthal as an inhibitor of HIV-1 Vpr induced cell death. Biochem Biophys Res Commun 2006;348:1101–6. https://doi.org/10.1016/j.bbrc.2006.07.158.

[16] Chen H, Muhammad I, Zhang Y, Ren Y, Zhang R, Huang X, et al. Antiviral Activity Against Infectious Bronchitis Virus and Bioactive Components of Hypericum perforatum L. Front Pharmacol 2019;10:1272. https://doi.org/10.3389/fphar.2019.01272.

[17] Zubek S, Mielcarek S, Turnau K. Hypericin and pseudohypericin concentrations of a valuable medicinal plant Hypericum perforatum L. are enhanced by arbuscular mycorrhizal fungi. Mycorrhiza 2012;22:149–56. https://doi.org/10.1007/s00572-011-0391-1.

[18] Fourneron J-D, Naït-Si Y. Effect of eluent pH on the HPLC-UV analysis of hyperforin from St. John's Wort (Hypericum perforatum L.). Phytochem Anal 2006;17:71–7. https://doi.org/10.1002/pca.888.